PROVISIONING THE NAKED ASTRONAUT WITH BOUNTY ON MARS using Robotic Self-Replicators

ALEX ELLERY[1] **& ANTHONY C. MUSCATELLO**[2] [1]Department of Mechanical and Aerospace Engineering, Carleton University, 1125 Colonel By Drive, Ottawa, Ontario, Canada, K1S 5B6; [2]Applied Sciences Branch, UB-R3-A, NASA, John F Kennedy Space Center, 32899 FL, USA

Email aellery@mae.carleton.ca

The high cost and risk associated with human Mars missions have been the primary barriers to their realisation. Much of this risk and cost can be alleviated by the emerging technology of machine self-replication. A single self-replicating machine may be launched and landed on Mars prior to the launch of astronauts. The seed may be envisaged as a 10-tonne mobile rover mounting a variety of machine tools to acquire regolith, rock and fluids from the Martian environment, process them and manufacture its various constituent components and assemble them. Thus, the self-replicator would spawn a population of universal constructing machines that would provide the astronauts with essential supplies on the Martian surface. A restricted set of raw materials from the Martian environment suffice to manufacture any kinematic mechanism from an array of derivative metals, ceramics and silicone plastics. Iron and its alloys form the centrepiece of this material technology. A universal constructor can by definition manufacture copies of itself thereby leveraging exponential productive capacity but it can also construct an entire Martian infrastructure prior to the arrival of astronauts. The key to realising such a self-replicating machine is the ability to 3D print electric motors and electronics. We shall show our developments in 3D printing electric motors. Our hypothesis is that if we can 3D print motors and electronics, we can print almost anything and transform human Mars exploration in terms of both cost and risk.

Keywords: Mars colonization, In-situ resource utilization, 3D printing, Self-replicating machines

1 INTRODUCTION

The exploration of Mars is a high priority for astrobiological research. Mars' early magma ocean solidified rapidly suggesting that Mars was habitable 100 My before Earth [1]. As the Martian magma ocean solidified, it yielded olivine, pyroxenes, garnet and ilmenite as per the Bowen crystallisation sequence. Outgassing of CO_2 and H_2O volatiles from the interior occurred during the magma ocean phase. The outgassed water vapour condensed into oceans after the magma ocean solidified within 20 My. The maximum greenhouse heating from a thick outgassed CO_2 atmosphere on Mars would have raised the average temperature of -60°C to -33°C. For liquid water to have flowed on the surface, CO_2 must have been supplemented with more powerful greenhouse gases such as CH_4 or the surface liquid water must have been salty to depress its freezing point to -55°C. It is expected that there are substantial water deposits underground in the form of hydrated basalts and regolith water ice at depths of 60-80 m [2].

Tracing water on Mars has been the mantra as a proxy for both the search for life and as a potential resource. It is suspected that the northern lowlands on Mars constitute a palaeo-ocean indicated by three palaeo-shorelines representing high ocean levels – Meridiani (Noachian), Arabia (Noachian) and Deuteronilus (Hesperian/Amazonian) shorelines – yet there is a lack of phyllosilicate, carbonate and evaporite deposits [3]. The Mars Express orbiter carried a spectrum of remote sensing instruments including those for the detection of subsurface water ice – high resolution stereo imager, infrared mapping spectrometer, UV/IR atmospheric spectrometer, planetary Fourier spectrometer, synthetic aperture radar and radio science. The Rosalind Franklin rover (2022) will carry a number of astrobiology-oriented instruments as part of its Pasteur payload served by a sample acquisition drill and a sample processing and distribution system – panoramic camera, infrared spectrometer, ground-penetrating radar, neutron spectrometer, drill cuttings close-up imager, in-drill infrared spectrometer, visual/infrared imaging spectrometer, Raman spectrometer and organic molecule analyser including a gas chromatograph/mass spectrometer. In both cases, the detection of subsurface ice is accomplished using ground-penetrating radar which measures differences between the dielectric properties (relative permittivity) of subsurface media. The interface between different materials such as regolith/ice results in partial reflection and partial refraction of the radar signal.

The Mars 2020 *Perseverance* rover will target the 45 km diameter Jezero palaeolake crater with detected clay deposits to drill for 30 samples of ancient microbial life. It will include, for the first time, a 1.8 kg Mars helicopter with 1.2 m span counter-rotating blades. Clays are indicative of former flowing water as they are aqueously deposited. The *Perseverance* rover is of the *Curiosity* class and will carry a suite of scientific instruments

An earlier version of this paper was presented at the 68th International Astronautical Congress, Adelaide, September 2017.

including 23 cameras, ground-penetrating radar, an X-ray spectrometer and a laser-induced breakdown spectrometer. It also includes an in-situ resource utilisation (ISRU) experiment to extract filtered carbon dioxide from the Martian atmosphere and convert it electrolytically into oxygen. *Perseverance* will seal the 30 samples in tagged canisters for later autonomous recovery by ESA's 2028 Mars "fetch" rover for return to Earth by a NASA Mars Ascent Vehicle (MAV) and an ESA Earth Return Vehicle (ERV) in 2031 [4]. The MAV may be fuelled with cryogenic LOX/LH_2 from derived from water for a specific impulse of 450 s. Human missions are expected to follow.

The high cost and risk associated with human Mars missions have been the primary barriers to their realisation. To address this, NASA has declared that any sustained human Mars exploration programme must: (a) be financially affordable; (b) provide incremental growth of mission capabilities; (c) possess an architecture that builds a Mars infrastructure for subsequent missions; and (d) offer private sector opportunities. It is our contention that a self-replicating system fulfills precisely these requirements. Much of the risk and cost can be alleviated by this emerging technology of self-replicating machines. Indeed, the proposed Mars colonisation phases – (i) Earth-reliance; (ii) Mars proving ground; (iii) Earth-independence – can be leap frogged directly to Earth-independence through self-replicating systems. Macroscopic self-replicating machines are a disruptive technology that would be transformative for space exploration in a way that no other technology can achieve. The power of self-replication technology to transform space exploration is immense, as it amortises initial capital launch costs over an exponential growth in productive capacity giving an exponentially decreasing specific cost [5]. The self-replicating machine concept is premised on autonomous operation. This robotic capability could serve to build entire infrastructures and expandable permanent facilities on Mars prior to human missions. Such self-replicating systems are founded on deep ISRU.

ISRU is built into almost all Mars exploration concepts. The NASA Human Mission to Mars Design Reference Architecture (HMMDRA) 5.0 is typical [6] but more recent visions have incorporated a degree of more philosophical musing [7]. In the latest NASA vision, it is envisaged that the Space Launch System (SLS) based on 4 Space Shuttle-derived engines will provide the mainstay of the human Mars programme expandable to a lift capability of 130 tonnes to LEO, 52 tonnes to cislunar trajectory or 41 tonnes to trans-Mars trajectory. The Orion capsule (or a Deep Space Habitat in more recent concepts) would accommodate a four-person crew for the trip for 500 days. A Mars ascent vehicle (MAV) delivered to the Martian surface would be fuelled with locally-derived methane and oxygen for return to Mars orbit to rendezvous with the Earth return vehicle (ERV). If the crew complement were increased to six astronauts with a more expansive capability, a 100-tonne payload allocation would be required including life support, scientific instrumentation, surface habitation and power generation systems. If the surface equipment can be manufactured in-situ, the life support for six astronauts would require only 20 tonnes dominated by water consumption of around 11 litres per day with recycling.

It is also envisaged that public-private partnership ventures will be implemented in Mars exploration. SpaceX has been an outstanding success with its contracts with NASA to deliver cargo to the ISS using its Dragon 2 capsule which is being expanded into its Red Dragon spacecraft for landing crews on Mars. The Falcon 9 rocket comprising 9 engines was first launched in 2010. The Falcon Heavy comprises three Falcon 9 stages with a lift-off thrust of 22,685 kN capable of landing 12.9 tonnes into a cislunar trajectory. In 2018, the SpaceX Falcon Heavy rocket launched a Tesla Roadster into interplanetary orbit beyond Mars – it has a payload capacity of 17 tonnes to Mars. SpaceX's re-usable Starship rocket will be designed to carry 150 tonnes to Mars. Elon Musk has proposed that a self-sustaining Mars colony of a million people could be established over the next few decades beginning in 2024. A cluster of 42 new Raptor engines using methane-liquid oxygen fuel would generate a lift thrust of 138,000 kN. The ship would be refuelled in LEO to transport 100 colonists (ticket price of $200,000) over a 90-day flight (mission cost of $10 B) to Mars. It would land on the surface vertically using retro-rockets in preparation for a return flight back to Earth. It would be refuelled using methane and oxygen manufactured in situ and would return to Earth for re-use. The Musk scenario would deliver astronauts "naked" to the Martian surface as it does not consider aspects of their survival once on Mars. This will almost certainly precede NASA's Space Launch System (SLS) – Orion capsule system to Mars.

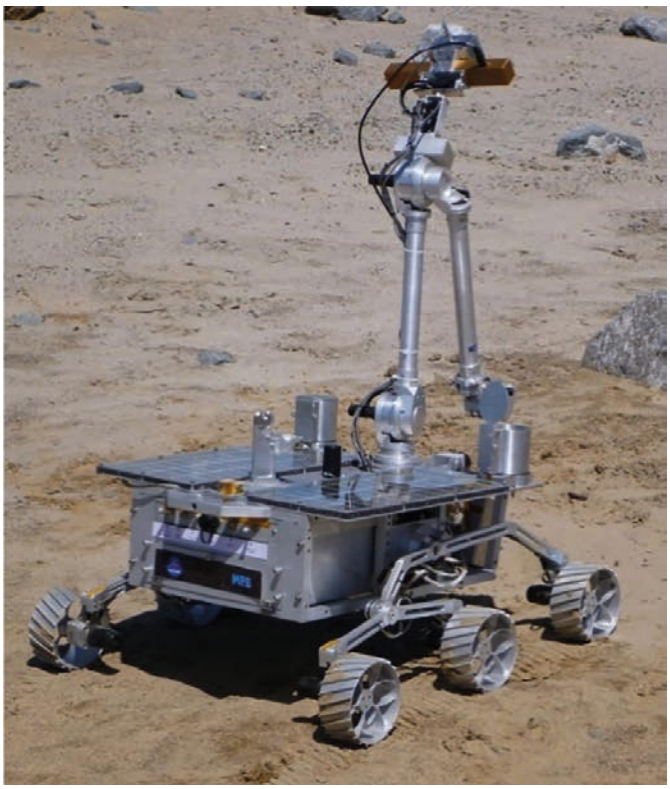

Fig.1 Six-wheeled *Kapvik* microrover at the Canadian Space Agency Mars Yard proving ground.

A piecemeal approach to ISRU does not exploit the synergies between ISRU, advanced additive manufacturing, and autonomous robotics enabled through machine learning to leverage the capacity of all these technologies as an ensemble. Self-replication absolutely requires this leverage between these technologies. We differentiate "deep ISRU" from "shallow ISRU" by virtue of the former's ability to build infrastructure capacity with minimal commitment from Earth rather than the supply of consumables. Deep ISRU enables the transition from fleeting exploration to full colonisation.

2 SHALLOW IN-SITU RESOURCE UTILISATION

Emphasis to date has been on shallow ISRU for the sound

reason that the greatest cost reduction to human Mars missions will be in in-situ propellant/oxygen/water supply. It is considered that recoverable water on Mars will have the most impact on human Mars exploration costs [8,9]. Many ISRU scenarios begin with physical extraction from the regolith. The Viking lander trench-digging and Sojourner wheel experiments indicated soil friction angles of 14-21°/28° for drift material, 27-33°/34-38° for blocky material and 28-39°/33-42° for crusty-cloddy material respectively. It is generally assumed that regolith friction angle equates to the regolith's angle of repose. Such terramechanics data will dictate the nature of drilling, bucketwheel excavation and/or earthmoving activities required for resource acquisition. An example of such a recovery strategy is the 32 kg *Kapvik* microrover that deploys a unique rover mast that mounts a soil scoop at its end effector and a panoramic camera at its elbow that provides direct line-of-sight to the scoop (Fig 1).

Kapvik employs a unique capability in determining regolith cohesion and friction angle parameters whilst on the move that can potentially detect water ice in the regolith [10].

We use "shallow ISRU" to emphasise the focus on consumables that require only simple chemical processing to support human life. Shallow ISRU involves exploiting the Martian atmosphere and water from the regolith to manufacture fuel and oxidant to supply both the return leg of a Mars mission and the landed colonists with rover propellant/oxidiser, etc. [11]. Mars ISRU technology is reviewed in detail in [12]. Shallow ISRU begins with the capture of atmospheric CO_2 at 7 mbar which is filtered to remove the ubiquitous airborne dust and purified to remove the 2.7% N_2, 1.6% Ar and 0.4% other gases [13]. For life support, buffer gases are required that will leak through airlocks, seals, etc. so this places a premium on recovering nitrogen and argon as well as oxygen regeneration [14]. The filtered gases are then compressed to ~1-5 atm prior to chemical processing. Solid state sorption pumps based on zeolite adsorption are commonly preferred for their lack of moving parts. They operate thermally by absorbing CO_2 when cold (at night) and releasing it when heated by solar energy (during daytime).

Exothermic Sabatier processing of atmospheric CO_2 requires hydrogen. Early scenarios assumed – impractically – that hydrogen feedstock would be imported to Mars from Earth. However, hydrogen may be sourced from Mars. The amount of water vapour in the Martian atmosphere is small at only 0.03%, its low concentration making extraction difficult. Water ice exists at polar regions above 60° latitude where water ice is close to water's triple point so water is stable only as ice. The permanent caps of water ice are huge water resources [15] – the northern cap of 1000 km diameter stretches to 80° latitude; the southern cap of 350 km diameter is much smaller. Both are highly localised where solar power generation will be challenging. Water ice-rich soil has been detected within 0.5 m of the surface at high latitudes and within 1.5 m of the surface at latitudes as low as 40°. Water ice is available in many near-equatorial and mid-latitudes in concentrations of up to 10% within 1-2 m of the Martian surface detected by their high local albedo and low thermal inertia. A very recent reanalysis of the data from the Mars Odyssey neutron spectrometer [16] indicates water ice may be located within 1.0 m of the surface in several regions at or near the equator. These hydrated minerals (2-13% water) at lower latitude represent the most promising water sources [17].

Water ice must be heated to sublime it into vapour to be captured and subsequently condensed under pressure at 1.4 kPa. The latent energy for vaporising water is 2256 J/g (0.63 kWh/kg) compared with its latent heat of melting of 336 J/g. The advantage of evaporation is that it purifies the water. Water may be accessed by auger to drill into the subsurface and use convective heating or microwave to evaporate water in-situ for collection at a cold trap on the surface. Microwave has deeper penetration than local heating. While the sublimation of ice to steam requires temperatures above 100°C at one atmosphere, water of hydration requires heating of regolith to temperatures of 600°C but above 450°C, perchlorates produce HCl contaminant. Alternatively, a solar mirror/lens or microwave transmitter may be passed over the soil to evaporate the water that is retained by a cold plate within a solar still, tent or skirt. Water as a source of hydrogen circumvents the high costs of transporting hydrogen tanks from Earth. Martian soil may also be beneficiated using high energy microwaves due to the high incidence of iron.

The Sabatier reaction requires a nickel or ruthenium-on-alumina catalyst (only the former is readily extractible from in-situ resources but the latter yields 94% efficiencies) to react with hydrogen at 250-300 °C and 0.85 bar and yields both methane fuel and water:

$$CO_2 + 4H_2 \rightarrow CH_4 + 2H_2O + \Delta E = -165 \text{ kJ/mol}$$

Once started up, the reactor requires no further energy input so the Sabatier reaction can be implemented in a steel pipe containing a Ni catalyst bed. Methane and water are readily separated through condensation. Water is electrolysed to recycle the hydrogen feedstock and yield oxygen:

$$H_2O \rightarrow H_2 + \tfrac{1}{2}O_2$$

Electrolysis is quite energy-intensive at 5.3 kWh/kg of H_2O. Once recovered, hydrogen is difficult to store and requires cryogenic treatment so it is best recycled continuously – methane does not suffer from this problem so represents a convenient means to store and use hydrogen as fuel. The total Sabatier/electrolysis process produces 75 kg of O_2 from 100 kg of CO_2 with close to 100% efficiency. It gives a 2:1 O_2:CH_4 ratio which may be increased to 4:1 (for a propulsive performance I_{sp} of 380s) by [18]:

(i) electrolysing native water ice or adsorbed/hydrate water from the regolith as proposed earlier;
(ii) electrolysing atmospheric CO_2 at 800-1000°C via a zirconia (ZrO_2) membrane ($2CO_2 \rightarrow 2CO + O_2$) through which oxygen is separated out without using hydrogen;
(iii) the inefficient endothermic reverse water-gas shift reaction reduces CO_2 to CO ($CO_2 + H_2 \rightarrow CO + H_2O + \Delta E = 41.2$ kJ/mol) with a Fe-Cr or Cu catalyst at 400-600°C followed by electrolysis of water (hydrogen is recycled). A Mars hopper that refuels itself for multiple hops using the CO/O_2 combination (I_{sp} of 250s) has been suggested as a demonstrator of this technology [19].

The first option is much preferable as hydrogen feedstock is available from Mars in several forms as discussed earlier. The oxygen produced may be compressed and stored cryogenically using a Stirling cycle refrigerator. An alternative fuel to CH_4 is to use CO_2 as an oxidiser with metal particles such as Mg as propellant with CO_2/metal in the ratio 2:1 offering an I_{sp} of 220 s. Acetylene fuel has a similar performance to methane (boiling point of -82°C compared with -165°C for methane) and may be produced through the pyrolysis of methane at 1250°C [20]: $2CH_4 \rightarrow C_2H_2 + 3H_2$. This can provide the basis for gas welding or cutting with oxygen. Although usually proposed for

fuelling only the MAV to an ERV in Mars orbit, the Sabatier/electrolysis-derived methane and oxygen can be exploited to manufacture propellant/oxygen on Mars for the entire return journey [21] though this would require refuelling of the ERV in Mars orbit. The Mars In-Situ Propellant Precursor (MIP) was a sophisticated flight demonstration package to extract O_2 from the Martian CO_2 that never flew [22]. It was based on an yttria-stabilised zirconia solid oxide electrolyser supported by solar array power, dust experiment, thermal radiators and air compressor. Oxygen was produced by solid state electrolysis of atmospheric CO_2 at a temperature of 900-1000°C. Thin discs of yttria-stabilised zirconia or doped ceria (CeO_2) were sandwiched between porous Pt metal electrodes and CO_2 diffused through the porous electrodes. CO_2 electrothermally dissociated into O_2 – ions that passed through the solid electrolyte to the anode where they were liberated as O_2. The solid electrolyte acted as the conductor of ions, in this case, negative oxygen ions through the holes in its doped crystal lattice in an applied electric field. The electric field was generated by the flanking porous Pt electrodes applying a potential difference. Its performance was based on the Nernst potential – the minimum electrical energy required to maintain electrolysis – determined by the difference between oxygen partial pressures either side of the membrane [23]:

$$E_0 = \frac{RT}{nF} \ln\left(\frac{P_a}{P_c}\right) \quad (1)$$

where R = gas constant, T= cell temperature, n = number of electrons transported per oxygen molecule, F = Faraday's constant, P = oxygen pressure on anode/cathode side. These ISRU technologies – Sabatier production of methane/water and water electrolysis production of oxygen – are directly applicable to ECLSS (environmental control and life support systems) as well as propellant/power production [24, 25].

An expert system will be particularly important for continuous operations and for the supply mission-critical resources such as oxygen for life support and fuel. It has been suggested that rule-based diagnostic expert systems using a dynamic chemical model would be suitable for ISRU systems [26]. The production process must be simple and robust to minimize human interaction. The simplest model assumes a continuous supply of reagents with controlled input flow mass and monitored output mass of both products and waste. Intermediate mass flows must also be monitored and regulated through operating conditions of flow rate, pressure, temperature, voltage and current – temperature in particular is a sensitive control variable. For gases such as in a Sabatier reactor, this is relatively simple. However, the Sabatier approaches to Mars ISRU are all limited to the manufacture of consumables, i.e. shallow ISRU. However, it may be possible to manufacture much of the MAV itself from local resources – the Terran 1 launcher with a simplified design is to be 3D printed using a custom multi-armed system that deposits liquid aluminium through direct laser melting of powder followed by finishing [27]. Thermal insulation may also be incorporated into Martian manufacture of the MAV. Silica aerogel used as high-performance thermal insulation has been direct ink write 3D printed from a pentanol-based solution of silica nanoparticles which solidifies into a highly viscous sol [28]. These capabilities might be replicated on Mars for 3D printing the MAV.

3 SELF-REPLICATION

Our technological tools constitute the extended phenotype of our species, without which we are naked. Without significant technological support, astronauts on Mars will be naked and unable to survive. To support the naked astronaut on Mars, a single self-replicating machine may be sent either prior to human arrival (the preferable option) or brought with the human element as the main infrastructure system. The former option is a variation on the Mars Direct and derivative scenarios: a single self-replicating machine may be launched from Earth and landed on Mars prior to the launch of astronauts. The self-replicating machine is a singular technological entity from which all other technological products may be manufactured by virtue of its universal construction property. It may be envisaged as a mobile rover mounting a variety of machine tools to acquire regolith, rock and fluids from the environment, process them and manufacture its various components and assemble them. On the Martian surface, the self-replicator initially manufactures copies of itself to reach the desired productive capacity. In the process, it manufactures infrastructure that may be co-opted to support the human mission such as load-haul-dump rovers, robotic drills, comminution/beneficiation machines, unit chemical processors, 3D printers, intelligent assembly manipulators, etc. Thence, once a desired population has been achieved, it manufactures products on-demand from in-situ resources including potentially the entire Mars Habitat, Mars Ascent Vehicle/Earth Return Vehicle from local resources (this may be accomplished prior to the launch of the human element to mitigate risk). The naked astronauts will also require provisioning with products and expanding the restrictive 20 m^3 living volume per colonist in the Mars interplanetary transport to a more tolerable 90 m^3 or more. The self-replicating machine would spawn a growing population of universal constructing machines that would provision the astronauts with essential supplies on the Martian surface. No astronaut should leave Earth without a self-replicating machine – its universal construction property ensures that it can construct an entire Martian infrastructure as well as consumables prior to the arrival of the astronauts.

Most self-replicating machine work to date has focussed on assembly processes, often using "Lego bricks" as a demonstration platform to eliminate complexities introduced by feedstock issues [29] – essentially, this is a variation on reconfigurable robotics using modular units [30]. Early work in self-replicating machines regarded in-situ manufacture of complex components and systems such as electric motors and electronics as too difficult [31]. They recommended that *such items should be supplied as prefabricated "vitamins" from Earth. We disagree and suggest that anything less than 100% self-replication is not self-replication rather than being partial replication that circumvents the most challenging aspects of replication. Indeed, we consider that motors and electronics are the "de facto" core of any self-replication capability.* This is illustrated by the original von Neumann kinematic model of self-replication that was based on two systems [32] – a motorised mechanical arm as a universal physical constructor and a universal electronic computer to sequence and control the arm. *The universal constructor is a machine that can be programmed by the computer to construct any other machine (including a copy of itself)* from resources in its environment. It was von Neumann's assertion that a universal constructor is sufficient for self-replication (on the basis that universal construction includes the construction of itself). Of course, this model assumed a robotic arm that functioned in a sea of constituent components from which to assemble a copy of itself. To incorporate mining and ISRU into the process, the robotic arm must be abstracted to include a variety of robotic devices – drills, mining rovers, pumps for driving chemical processes, 3D printers (which are essentially Cartesian robots),

milling machines, etc. All these kinematic machines constitute different kinematic configurations of electric motors and all are motorised systems controlled by electronic circuits comprised of a finite set of electronic components.

There has been interest recently in deploying new 3D printing technologies in space to create static structures – all involve the use of plastic either as the primary material [33] or as binder with local regolith [34]. 3D printing is a fast-developing manufacturing technology that has yet to attain its full potential, currently restricted to the manufacture of static structures, albeit useful for habitat construction. Inspired by the RepRap 3D printer [35], the ability to 3D print robotic components – actuators, electronic circuitry and sensors – will demonstrate that 3D printing constitutes a universal construction mechanism in the spirit of von Neumann. Other robotic mechanisms can also be built including powered machine tools, 3D printers, rovers, manipulators, drills, etc. from which almost anything can be constructed and assembled. The electric motor and the vacuum tube provide the key components for actuation and electronics respectively, both constructed from a small set of materials derivable from Martian resources. The corollary of this is the ability to build robotic machines and all the subsystems of a spacecraft on-demand. We have discussed a self-replicating machine in the context of the Moon [36] but our approach is bottom-up and differs from the top-down approach proposed in [37]. In addressing the manufacture of the basic components for a self-replicating machine – motors and vacuum tubes – we must invoke deep ISRU. We do not consider biological issues regarding ISRU other than to suggest that the Mars environment may offer a suitable habitat for their exploitation.

4 DEEP IN-SITU RESOURCE UTILISATION

Mars is hostile to human habitation. It will be essential to exploit Mars resources through deep ISRU for the colonists to survive. The bottom-up approach to self-replication begins with a restricted set of raw materials from the Martian environment. It is unlikely that the scientific search for extant or extinct life on Mars per se will be a sufficient spur for the human exploration of Mars [38]. However, ISRU to support human colonisation of Mars will require intimate knowledge of Martian geology including its astrobiological context. Most lunar ISRU techniques apply to Mars characterised by extensive water ice for hydrogen and atmospheric CO_2 as a plentiful carbon source for the Fischer-Tropsch manufacture of plastics and rubbers while NaCl salts are extensively distributed as a source of chemical reagents such as HCl acid.

The Martian surface comprises primarily of basalts, dominated by Si, Ti, Al, Fe, Mg, Ca and Na plus other lesser elements K, Cr, Mn, P, S and Cl. The basaltic crust comprises variable amounts of plagioclase feldspar, pyroxene and olivine with Fe oxides [39]. The distribution of minerals pyroxene (as coexisting clino- and ortho-pyroxenes), plagioclase and olivine is widespread and there is evidence of magmatic differentiation with silica-rich quartz and feldspars [40]. Martian basalts have higher Fe_2O_3 content than terrestrial basalts. Martian regolith is also iron-rich including iron oxides/(oxy)hydroxides including haematite, goethite, ferrihydrite, spinels (such as magnetite and titanomagnetite), maghemite, lepidocrocite, akageneite, schwertmannite and feroxyhyte – of which haematite and goethite are the most abundant. SNC meteorites indicate that Mg, Al, Ti, Fe and Cr are common with trace amounts of Li, Co, Ni, Cu, Zn, Mo and W on Mars. However, the Martian surface lacks aluminium-rich anorthositic deposits due to its high-pressure interior favouring the formation of garnet as the main repository of aluminium. Sulphur is enriched compared to Earth due to extensive sulphate salts deposited during the Hesperian including jarosite ($(K,Na,H)Fe_3(SO_4)2(OH)_6$), gypsum ($CaSO_4.2H_2O$) and kieserite ($MgSO_4.H_2O$). Magnesium sulphates in particular are promising indicators of potential halophilic habitats [41]. There exist other halides indicative of evaporitic deposits. Chloride, sulphate and carbonate brines in regolith appear to be ubiquitous near the surface of Mars as evidenced by the recurrent slope linea that occur in the spring/summer due to brine flows. The brines have lower freezing temperature than water so they can remain liquid in the Mars regolith. The surface of Mars is highly oxidised including the incidence of perchlorates – perchlorate brines have freezing temperatures of -70°C.

Phyllosilicates (clays) – smectite, montmorillonite, kaolin and serpentine – are ubiquitous on Mars indicating substantial water flows on the surface during Mars' first 500-700 My [42]. For example, minnesotaite is an iron-rich talc product of weathered fayalite. Clays including Fe-rich (nontronite), Mg-rich (saponite) and Al-rich (montmorillonite) varieties have been detected on the southern Noachian crust. They resulted from aqueous activity in Noachian exposures during the formation of the river valley networks. Palaeolakes existed during late Noachian-early Hesperian epoch when salts – NaCl, $MgCl_2$, $CaSO_4.nH_2O$ (gypsum), $MgSO_4.7H_2O$ (epsomite) and $KFe_3(OH)_6(SO_4)_2$ (jarosite) were laid. Gypsum has been detected as veins deposited by circulating fluids. Martian soils have high concentrations of S and Cl suggesting sulphate and chloride salts over widely spaced geographical locations – these elements are depleted on the Moon. Haematite deposits such as the blueberries date from the Hesperian due to hydrothermal circulation during outflow channel formation. An apparent frozen body of ice in Elysium was emplaced near the equator as recently as 5 My ago, but the most recent volcanic activity in the Tharsis/Elysium region was estimated to have been 100-200 My ago. Nevertheless, there is evidence of glacial deposition at Olympus Mons some 5 My ago indicating that Mars' spin axis was more oblique than today. Elysium would be an obvious target for its water ice inventory. Mars exhibits sedimentary deposits that have been concentrated by hydrothermal fluids from volcanic, tectonic and impact heating [43]: (i) the Tharsis bulge is a 10 km high large igneous province (LIP) some 4000 km in diameter formed by a mantle plume beneath the stationary single tectonic plate; (ii) on its northwest region are three large shield volcanoes and further northwest lies the 550 km diameter by 24 km high Olympus Mons, the largest shield volcano in the solar system; (iii) the 4000 km long by 600 km wide by 10 km deep Valles Marineris is the largest rift canyon in the solar system; (iv) the 2100 km diameter by 9 km deep Hellas impact crater is ringed by a 2 km high rim.

LIPs are typically associated with useful chalcopyrite and siderophile elements including Ni-Cu-PGE (platinum group elements), Ti, Fe, Cr, etc. On Earth, LIP are large, thick accumulations of igneous rock (typically 20-40 km thick over thousands of square km), especially iron-magnesium rich basalt, and are commonly created by continental flood basalts, giant oceanic plateaus and volcanic rifted margins due to deep mantle plumes from the core-mantle boundary erupting at hot spot locations over geologically short periods ~105-106 y [44], e.g. Deccan Traps, India over 5 x 10^5 km^2 formed just prior to the unrelated KT impact event 66 My ago. They are often associated with mass extinction events due to the release of massive amounts of sulphate aerosols rather than carbon dioxide [45], e.g. the Si-

berian Traps correlate with the Permian-Triassic mass extinction. They are often associated with concentrated deposits of copper-iron-nickel and platinum group metals. Hydrothermal convection associated with volcanoes form massive sulphide deposits of Cu, Zn, Pb, etc. Some haematite deposits may be deposited similarly (though haematite blueberries are surface aqueous deposits). Impacts are known to result in Cu-Ni-PGE deposits with hydrothermal fluid deposition of Cu, Zn, Pb, etc mineral veins, e.g. Sudbury crater. Hence, identifying LIP offers potentially valuable ore locations.

The most obvious in-situ resource to exploit on the surface of Mars by the colonists is Martian regolith. Duricrete – a weak version of concrete – may be made by wetting and drying the soil which contains high amounts of Ca such as gypsum (5% on average). Basalt may be melted above 1100°C and extruded into layers for 3D printing large-scale pressurised structures [46] – Duricrete has a modulus of elasticity of 70 GPa and a tensile strength of 14 MPa. Glass-ceramics may be formed from powdered basalt melted at 1250-1550°C and then cooled to 800-950°C for nucleation into a mixed crystalline/glass phase [47]. The microstructure is determined by the cooling schedule. High TiO_2 concentration promotes nucleation and increases viscosity while high Fe_2O_3 concentration decreases viscosity [48]. Furthermore, plagioclase should be avoided, favouring the extraction of low concentrations of alumina (Al_2O_3) and quicklime (CaO) for high strength glass-ceramics. More intriguingly, D-shape is a means of 3D printing regolith to form an outer protective shell to a habitat structure to provide protection from environmental radiation [49]. The 3D printer for D-shape is a large 3 degree-of-freedom Cartesian frame moving a printing head/regolith spreader blade mounted onto a beam. The printing head comprises 300 nozzles across a 6 m beam which selectively sprays ink to bind the regolith at certain locations. The low viscosity ink comprises two parts: (a) 15-30% MgO dissolved in water forming $Mg(OH)_2$; (b) a saturated solution of magnesium chloride hexahydrate ($MgCl_2.6H_2O$). When mixed together, the two components react exothermically to form the fast-setting Sorel cement $Mg_4Cl_2(OH)6(H_2O)_8$ which binds regolith into 70 MPa compressive structures (though much inferior to basalt for load-bearing). Unlike on the Moon, sulphur (in the form of gypsum) and chlorine (in sodium and magnesium salts) from evaporate deposits are ubiquitous in Martian soil. Forsterite (Mg_2SiO_4), a common olivine mineral on Mars (and the Moon), may be treated with HCl directly to yield silicic acid and $MgCl_2$:

$$Mg_2SiO_4 + 2HCl \rightarrow 2MgCl_2 + H_2SiO_4$$

Silica may be precipitated out from silicic acid leaving water. MgO powder may also be extracted from olivine which is readily dissolved:

$$Mg_2SiO_4 + 4H_2O \rightarrow 2MgO + SiO_2 + 4H_2O \text{ (forsterite)}$$

The salt $MgCl_2$ may be mixed with local supplies of water and MgO powder to form the binder. $MgCl_2$ may also be generated via HCl treatment of MgO:

$$MgO + HCl \rightarrow MgCl_2 + H_2O$$

However, the use of Mars regolith as a radiation shielding for surface habitats may be of limited effectiveness against galactic cosmic rays and solar flare activity due to the poor natural shielding of the thin Martian atmosphere [50]. In transit, a mission to Mars with 2 g/cm^2 of Al spacecraft shielding exposes the crew to a radiation dose of 15 rem/y at solar minimum and 31 rem/y at solar maximum. A 500-day sortie on Mars exposes astronauts to only 120 mSv but the six-month outbound/inbound journey will increase this to 1 Sv in total – sufficient to increase the risk of cancer in a 40-year old to 4%. Native gypsum may be exploited to manufacture cement or concrete which, by virtue of its high water content, provides effective radiation shielding. Gypsum ($CaSO_4{\cdot}2H_2O$) when heated to 150-200°C yields gypsum plaster (plaster of Paris – $CaSO_4$):

$$CaSO_4.2H_2O \rightarrow CaSO_4.½H_2O + 1.5H_2O$$

When mixed with water, the dry powder reforms into gypsum as a binding agent that hardens. Gypsum may act as a source of lime through more thorough heating for use in cement:

$$CaSO_4.2H_2O \rightarrow CaSO_4 + 2H_2O \rightarrow CaO + SO_2 + ½O_2$$

The resultant clinker is ground into a powder. The addition of water to quicklime (CaO) forms a slaked lime ($Ca(OH)_2$) paste. When exposed to atmospheric CO_2, $Ca(OH)_2$ slowly hardens to $CaCO_3$. In Portland cement manufacture, which is also suitable for Mars, CaO is mixed with clay to form 65% CaO, 23% SiO_2 and 4% Al_2O_3. When mixed with water, it forms calcium silicate hydrate which hardens. The evolved SO_2 from gypsum may be captured and converted into sulphuric acid as a reagent. Troilite may be roasted and oxidised as an alternative source of sulphur:

$$2FeS + {}^7/_2O_2 \rightarrow Fe_2O_3 + 2SO_2$$

With 75% aggregate, cement becomes concrete. Concrete is stable with a high compressive strength >100 MPa across a wide temperature range of -150°C to 600°C. Concrete can be reinforced with metal or glass fibres to increase its strength. MDF (macro-defect-free) is a high-performance cement that uses only small quantities of water but requires a water-soluble polymer. It requires roll-mixing to eliminate gas bubbles, dry curing at 80°C and may be extruded and moulded like plastic. DSP (densified with small particles) cement offers marginally inferior performance but does not require polymer and does require more water.

Our concern here is less with static civil engineering structures (for factory facilities) and more with the ability to construct robotic machines from local resources – such machines are matter amplifiers in leveraging local resources. A restricted set of key materials – iron, nickel, cobalt, tungsten, selenium, silicon, carbon, hydrogen and chlorine – suffice to manufacture any kinematic mechanism from an array of derivative metal alloys, ceramics and silicone plastics (Table 1).

Iron and its alloys form the centrepiece of this material technology – it is unnecessary to extract aluminium. Useful minerals include pyrite (FeS_2), ilmenite ($FeTiO_3$), haematite (Fe_2O_3), goethite (FeO(OH)), and hydrated silica (SiO_2). Nickel-iron meteorites provide a source of further metals including nickel and cobalt. Iron oxides and meteoritic iron, nickel and cobalt may be concentrated from gangue electrostatically and magnetically. Electrostatic separation requires a motorised drum while magnetic separation requires the use of magnets, both motor-derived capabilities – of crucial importance with regard to demonstrating that motor manufacture contributes to universal construction capability. NASA's PILOT (Precursor ISRU Lunar Oxygen Testbed) uses a motorised tumbling reactor to

TABLE 1: Mars-derived functional materials requirements

Functionality	Traditional Materials	Mars Substitutes	Applications
Tensile structures	Aluminium alloy, iron alloys (steel), titanium alloy, plastic, composite materials	Wrought iron, cast iron, steel	General structures including vehicles
Compressive structures	Concrete/cement	Regolith, cement/concrete, basalt	Buildings/fixed infrastructure
Elastic structures	Metal springs/flexures, rubber	Iron alloy springs/flexures, silicone elastomers	Compliant structures
Thermal conductors	Aluminium, copper heat pipes	Steel, fernico	Thermal straps, radiator surfaces
Thermal insulation	Glass (fibre), ceramic	Glass (fibre), ceramic	Thermal isolation
Thermal tolerance	Tungsten, tantalum	Tungsten	Vacuum tube electrodes, high temperature crucibles
Electrical conduction	Aluminium, copper, nickel	Fernico (e.g. kovar), nickel	Electrical wiring, resistors, capacitors, inductor coils, motor coils, electromagnet coils
Electrical insulation	Glass, ceramic, plastic, silicon steel	Glass, ceramic, silicone plastic (to be minimised), silicon steel	Vacuum tube enclosures, ceramic plates (motor cores and capacitors), plastic sheathing, electric motor cores
Active electronics	Solid state	Vacuum tubes (kovar, nickel/steel, tungsten, glass)	CPU, op-amps, solar cells
Magnetic materials	Rare earth materials (permanent magnets), Supermalloy	Silicon steel/laminate (electromagnets), Permalloy,	Magnetic flux generation (motors), magnetic shielding
Sensors and sensory transduction	PVDF/PZT, PN junction semiconductors	Quartz, selenium, thermionic conversion	RF oscillators, electricity generation, optical vacuum tubes (photodiodes and photomultipliers)
Optical structures	Polished aluminium, glass	Polished nickel, glass	Mirrors, lenses, optical fibres
Liquids	Hydrocarbon oils	Water, silicone oils	Lubricants, hydraulic force transmission (e.g. hot isostatic pressing), coolant
Gases	Air – petrol/paraffin	Oxygen – methane	Oxidant – propellant

mix and heat lunar regolith (dominated by ilmenite $FeTiO_3$) to 800-1000°C in the presence of hydrogen [51]. A similar approach may be applied to Martian haematite:

$$Fe_2O_3 + 3H_2 \rightarrow 2Fe + 3H_2O$$

The water produced is electrolysed and the hydrogen recycled. In this way, iron-bearing minerals are reduced to release oxygen. Reduction of Martian iron oxide such as haematite to pure iron is better achieved by carbothermic reduction using CO gas rather than H_2 because its ready derivation from abundant CO_2 on Mars:

$$Fe_2O_3 + 3CO \rightarrow 2Fe + 3CO_2 \text{ at } 1200°C$$
$$Fe_2O_3 + 3C \rightarrow 2Fe + 3CO \text{ at } >1200°C$$

Carbothermal reduction is similar to the reduction of iron oxide in electric furnaces on Earth. Haematite may be readily converted into magnetite under hydrothermal conditions at 350-750°C/1-2 kbar [52]:

$$3Fe_2O_3 + H_2 \leftrightarrow Fe_3O_4 + H_2O$$
$$4Fe_2O_3 + Fe \leftrightarrow 3Fe_3O_4$$

There are a number of steels (Fe 18.5% Ni, 8.5% Co, 5% Mo and <2% C) that may be manufactured on Mars: (i) tool steel (0.85% C + 4.15% Cr + 0.35% Mn + 5% Mo + 0.3% Si + 6.4% W + 1.95% V); (ii) spring steels (0.9-1.03% C + 0.3-0.5% Mn); (iii) shock-absorbing steel (0.5% C + 1.5% Cr + 2.5% W); (iv) stainless steel (0.95-1.2% C + 16-18% Cr + 0.65% Mo). These require the extraction of further metals that may be sourced from nickel-iron meteorite ores which are expected to be in an oxidised state:

$$Co_3O_4 + 4H_2 \rightarrow 3Co + 4H_2O$$
$$NiO + H_2 \rightarrow Ni + H_2O$$

If nickel and cobalt in nickel-iron meteorites are in a reduced state, they may be extracted through the carbonyl (Mond) process using a sulphur catalyst:

$$Fe(CO)_5 \leftrightarrow 5CO + Fe \text{ (175°C/100 bar)}$$
$$Ni(CO)_4 \leftrightarrow 4CO + Ni \text{ (55°C/1 bar)}$$
$$Co_2(CO)_8 \leftrightarrow 8CO + 2Co \text{ (150°C/35 bar)}$$

The discovery of several nickel-iron meteorites on Mars in close proximity to the Mars Exploration Rovers indicate their widespread incidence as a supplement to blueberry deposits of haematite for the production of steel alloy with small amounts of carbon extracted from the CO_2 atmosphere [53]. Furthermore, nickel-iron meteorites are a source of nickel, cobalt, tungsten and selenium for steel alloy production and other applications. Although nickel-iron meteorites appear to be common on the Martian surface, some drilling may be necessary. The husbanding of meteoritic resources may best be implemented as part of a global supply infrastructure serving the machine population

rather than within each self-replicating unit.

We consider the common steel additives: (i) C is widely available on Mars and may be cracked from $CO_2 + 2H_2 \rightarrow C + 2H_2O$ with an Fe catalyst at 650°C (Bosch process); (ii) Ni increases the strength and toughness of the alloy but not hardness – this is recoverable from nickel-iron meteorites; (iii) W controls the grain structure for providing high hardness for edges – tungsten grains are recoverable from nickel-iron meteorites; (iv) Si improves hardening of the alloy – this is recoverable from silicate-derived silica; (v) Mo increases the hardness and toughness of the alloy and improves corrosion-resistance to rusting – hardness is implemented with Si, toughness with Ni and Mars has no exposure to liquid water/oxygen making the Mo additive unnecessary; (vi) Mn is a deoxidiser additive which is unnecessary in non-oxidising extraterrestrial environments such as Mars; (vii) P imparts resistance to oxidative corrosion which is unnecessary in non-corrosive extraterrestrial environments such as Mars (except perhaps regarding the highly oxidised surface regolith); (viii) Cr increases the depth of surface hardening at the cost of increasing the tendency to cracking and creates resistance to iron oxide-formation – this is a non-essential additive; (ix) V retards grain growth to control the grain structure during heat treatment – this can be replaced with additive manufacturing process control; (x) S is an impurity that must be minimised so contamination by FeS must be avoided. Hence, we can create a family of steels using a handful of alloying elements readily recoverable from the Martian environment that offers sufficient if not optimised functional properties.

Ore bodies may also have formed on Mars due to hydrothermal processes. For instance, copper sulphide appears to be localised into ores rather than ubiquitous. We assume that it is not readily accessible. Copper as an electrical conductor can be substituted by kovar (a fernico alloy comprising 53.5% Fe, 29% Ni, 17% Co, 0.3% Mn, 0.2%Si and <0.01% C) or nickel (with a conductivity of $1.4x10^7$ S/m compared with $3.5x10^7$ S/m for Al) to reduce the complexity of mining and processing.

The weathering of olivine in water in the presence of CO_2 gas yields serpentinite and magnetite:

$$(Fe,Mg)_2SiO_4 + nH_2O + CO_2 \rightarrow Mg_3Si_2O5(OH)4 + Fe_3O_4 + CH_4$$

This reaction is favoured in low CO_2 environments and/or with Mg-poor minerals. Under all other conditions such as those on Mars, the reaction yields silica:

$$(Fe,Mg)_2SiO_4 + nH_2O + CO_2 \rightarrow Mg_3Si_2O_5(OH)_4 + Fe_3O_4 + MgCO_3 + SiO_2$$

A second reaction permits simple recovery of $MgCl_2$ by reaction with HCl (for Sorel cement):

$$MgCO_3 + HCl \rightarrow MgCl_2 + H_2O + CO_2$$

The olivine fayalite may be artificially weathered with water to yield magnetite and silica (as described earlier):

$$3Fe_2SiO_4 + 2H_2O \rightarrow 2Fe_3O_4 + 3SiO_2 + 2H_2O$$
(fayalite magnetite)

Salt may be used to create sodium carbonate (via the Solvay process) which may be dissolved in silica solution at 350°C and 150 MPa to grow quartz (over 40-80 days):

$$2NaCl + CaCO_3 \leftrightarrow Na_2CO_3 + CaCl_2$$
$$Na_2CO_3 + SiO_2(i) \leftrightarrow Na_2SiO_3 + CO_2$$

Quartz is piezoelectric and may be employed in a wide variety of fundamental sensor functions – displacement, pressure/force/acceleration, weight, etc. – and as crystal oscillators in radiofrequency electronics. A high frequency oscillator also provides the basis for ultrasound generation which projects high frequency vibrations into material. Additionally, the ultrasonic motor comprises a piezoelectric stator and a rotor driven by resonant displacement based on friction [54] and the piezoelectric stack-driven percussion-based ultrasonic/sonic driller/corer (USDC) penetrates igneous rock [55] which may be exploited but we have assumed traditional electric motors as the primary means to motive power.

One method of producing metals from regolith is molten regolith electrolysis (MRE). Studies have demonstrated the production of Fe metal and FeSi alloy as a byproduct of the generation of oxygen from simulated regolith by electrolysis at high temperatures (1600°C) [56, 57]. Few materials can withstand and contain molten regolith and metal product temperatures so the regolith itself is used to prevent destruction of the container. Counter gravity (CG) (vacuum moulding) of the liquid metal product can be used to obtain fairly pure metal or alloys for further processing and use.

The FFC Cambridge process offers a generalised electrolytic process to reduce mineral oxides to pure metal [58]. It uses a $CaCl_2$ electrolyte at 900°C with a sintered cathode formed from powdered metal oxide and a graphite anode. The cathode is reduced to >99% pure metal electrolytically. On Mars, the existence of perchlorates [59] may be exploited as a supply source of electrolyte. Magnesium perchlorate decomposes at 420-440°C in a vacuum:

$$2Mg(ClO_4)_2 \rightarrow MgO + MgCl_2 + 3.5O_2 + 2Cl$$

$MgCl_2$ may be reacted with calcium hydroxide to form $CaCl_2$ electrolyte for resupplying the FFC Cambridge process:

$$MgCl_2 + Ca(OH)_2 \leftrightarrow Mg(OH)_2 + CaCl_2$$

This makes the FFC Cambridge process viable as part of a self-replicating system – it can reduce haematite, rutile, alumina, silica, etc. directly into pure elemental metals subject to other contaminants.

Syngas for the manufacture of plastic may be derived from the reverse water-gas shift reaction by feeding H_2 in a 3:1 ratio to CO_2:

$$6H_2 + 2CO_2 \rightarrow 2H_2O + 2CO + 4H_2$$

The exothermic Fischer-Tropsch reaction involves the hydrogenation of CO at 320°C and is used to produce straight chain alkane hydrocarbons of the form CnH_2n+2 [60]:

$$(2n+1)H_2 + nCO \rightarrow CnH_2n+2 + nH_2O$$

When n=1, methane is produced. Alkenes are also produced as side reactions:

$$2nH_2 + nCO \rightarrow CnHn + nH_2O$$

Methane may be subject to oxidative coupling to yield ethylene exothermically at 800-950°C [61]:

$$2CH_4 + O_2 \rightarrow C_2H_4 + 2H_2O + \Delta H=-280 \text{ kJ/mol}$$

This is the starting point for the manufacture of plastics from ethylene. Ethylene (and higher plastics) can also be manufactured through the Fischer-Tropsch reaction in the presence of Fe, Ni or Co catalyst:

$$2CO + 4H_2 \rightarrow C_2H_4 + 2H_2O$$

The Fischer-Tropsch reaction requires a H_2:CO ratio of 2 (using a Co catalyst nominally but Fe catalysts can tolerate a lower ratio) and the H_2:CO may be altered through the water-gas shift reaction to increase the H_2 component:

$$H_2O + CO \rightarrow H_2 + CO_2$$

Clays have been detected in Noachian terrain due to aqueous action on silicate minerals by weathering or hydrothermal sources. Fe-Mg smectite clays have been detected in SNC meteorites resulting from the alteration of olivine. Clays may be exploited as organic catalysts – they are aluminosilicates comprising tetrahedral layers of SiO_4 bound to octahedral layers of AlO_6 by van der Waals forces. The interlayers of positive cations Ca, Na, Fe or Mg can become hydrated and expand the distance between the layers. Clays act as solid acids as they contain both Bronsted and Lewis acid sites [62] – Bronsted sites are associated with the interlayer sites while Lewis acids are associated with edge sites. Clays can bind organic molecules within their interlayers. Clay minerals in their use as catalysts for biochemical reactions form three groups – 7 Å unit kaolinite group, 10 Å illite group and 14 Å montmorillonite group [63]. Kaolin comprises layers of silica bonded to layers of alumina derived through the chemical weathering of potassium feldspar. Montmorillonite is formed from the weathering of ferromagnesian minerals such as pyroxene under hydrothermal conditions. On Mars, chemical weathering of pyroxenes at pH~3-4 proceeds more rapidly than that of feldspar so basalt is enriched in feldspar [64]. Artificial weathering of pyroxene may be implemented to yield montmorillonite and silica on demand:

$$Ca(Fe,Al)Si_2O_6 + HCl + H_2O \rightarrow Ca_{0.33}(Al)_2(Si_4O_{10})(OH)_2.nH_2O + H_4SiO_4 + CaCl_2 + Fe(OH)_3$$

Montmorillonite has a large number of uses including: (i) a catalyst; (ii) a component of drilling mud (bentonite is dominated by montmorillonite) to increase its viscosity; (iii) foundry sand binder for casting; and (iv) clay pottery. Montmorillonite ($Al_2Si_4O_{10}(OH)_2.nH_2O$) clays in particular are effective catalysts for many organic reactions such as the Diels-Alder reaction, Friedel-Crafts reaction, Friedlander synthesis, esterification reactions, porphyrin synthesis, polymerisation, etc [65, 66]. Lunar dust has been demonstrated as an effective catalyst for Fischer-Tropsch synthesis [67].

Plastics have a wide variety of applications including stiff structures, flexible structures (including inflatable structures), lubricants, sealants and adhesives. Although manufacturable from Mars volatiles, plastic is not an adequate structural material because of its sensitivity to radiation and limited temperature tolerance. While organosilizanes are used for specialised protective coatings and adhesive cements, radiation and temperature-tolerant organosiloxanes are used more widely – motor lubricants, motor insulation, sealants, adhesives and coolant. This favours siloxanes (silicone plastics) for their wide functionality. There are plastic pre-ceramic resins that can be 3D printed as plastic gel into structures which are then fired into a high temperature ceramic releasing much of its organic component [68]. Silicone plastics are one such type of pre-ceramic resin – polymer-derived silica-based ceramics are derived from pyrolysis of silicone polymers [69]. This permits shaping or 3D printing of the polymers prior to thermal conversion into ceramics offering high temperature stability to 1500°C (increased to 2000°C with the addition of Al using the sol-gel process). Polysiloxanes ($RSiO_{1.5}$) can also be transformed into piezoresistive SiOC ceramics through pyrolysis in an inert atmosphere at or above 1400°C – the high temperature is necessary for piezoresistivity with an extremely high sensitivity of ~145 [70]. Hence, ceramic structures can be 3D printed in polymer form. Silicone plastics manufacture begins with syngas. Methanol is synthesised from syngas through an exothermic reaction using an alumina catalyst:

$$CO_2 + H_2 \rightarrow CH_3OH$$

Chloromethane may be formed by heating methanol and HCl vapours at 350°C using an alumina catalyst:

$$CH_3OH + HCl \rightarrow CH_3Cl + H_2O$$

Chlorosilanes are synthesised through the Rochow process by passing methyl chloride (CH_3Cl) gas through solid Si powder bed at 250-300°C at 1-5 bar:

$$xSi + yCH_3Cl \rightarrow R_2SiCl_2 + H_2$$

Finally, the simplest silicone oil, polydimethylsiloxane (PDMS) is formed by hydrolysis:

$$n(CH_3)2SiCl_2 + nH_2O \rightarrow ((CH_3)2SiO)_n + 2nHCl$$

HCl is recycled. Higher silicone plastics may be manufactured similarly. Silicone plastic is ideal for flexible insulation for wire coils, electrical circuits and wiring harnesses. Silicone plastic may be 3D printed into layers through fused deposition modelling (FDM). Once laid, silicone may be then converted to silica by flame combustion in oxygen:

$$SiO_xC_y + (1-x+2y)O_2 \rightarrow SiO_2 + yCO_2$$

This provides a mechanism for 3D printing ceramics without involving extreme temperatures of direct sintering of ceramics. SiO_2 may be converted into its carbide form at 1200°C:

$$SiO_2 (s) + 3C (s) \rightarrow SiC (s) + 2CO (g)$$

This resembles geopolymer composites – heat-resistant polymerised oligosialates that involve matrices based on polymineral (aluminosilicate) resins [71]. Geopolymers are manufactured from metakaolin produced from the dihydroxylation of kaolin at 650-800°C. These binders are processed at a temperature range of 80-120°C similar to the temperature tolerance of plastic thermosettings but once polymerized, they can resist temperatures up to 1200-1500°C. Silica-based geopolymer binder is a polysialate structure (Si-O-Al-O) whose S:Al ratio determines its properties. A low ratio creates molecular networks whereas larger ratios are more polymeric. For example, (Na,K)-n(Si-O-)-(Si-O-Al-) has a Si:Al ratio >20. Geopolymer cement cures more rapidly than Portland cement at room temperature.

Glass or SiC fibre reinforcement of aluminosilicate geopolymers potentially offer reduced brittleness. The most common glass is soda lime glass containing 75% SiO_2, 15% Na_2O, 10% CaO and 2-3% additional material. In terrestrial glass, ground silica is mixed with specific amounts of iron, potassium and sodium oxide particles from feldspar, limestone and soda ash and heated to 1500°C. Soda and silica are the dominant constituents (usually with other additives such as soda-lime, borosilicate, etc. to reduce the glass melting point to 860°C) of terrestrial glass for ease of shaping:

$$(0.5\text{-}0.8)Na_2O + SiO_2 \rightarrow Na_2SiO_3$$

However, the significant amounts of FeO in Martian minerals will cause darkening. Hence, Fe must be removed magnetically or electrostatically. Glass may be cast as molten glass in a mould of clay-bound sand or metal. Investment casting involves a model of low-melting point material from which a clay investment mould is made. The investment cast is heated in a kiln in the presence of glass particles which melt into the mould. Glass plate may be formed by rolling glass from molten and trimming while soft.

Zeolites are microporous crystals of hydrated aluminosilicate minerals of alkaline or alkaline earth metals of the form $M_{x/n}[AlO_2)_x(SiO_2)_y].wH_2O$ where M = alkaline or alkaline earth metal, n = cation valence, w = number of water molecules, x+y = number of tetrahedral, y/x = 1-5 typically. Four AlO_4 and SiO_4 tetrahedra are joined by sharing O ions. Zeolite pore sizes vary from 0.3-1.0 nm with a volume of 0.1-0.35 cm^3/g. They act as molecular sieves that are often used as absorbents, catalysts and ion-exchange beds [72]. Zeolites are formed naturally where volcanic rock reacts with alkaline groundwater. Zeolites may be formed synthetically by heating aqueous solutions of alumina and silica with NaOH forming sodium aluminate and sodium silicate [73]. Hence, they can be manufactured on Mars. A common zeolite is zeolite A of the form $[Na_{12}(H_2O)27][Al_{12}Si_{12}O_{48}]$ [74]. Zeolite A may be synthesised by mixing kaolinite clay with NaOH at 800°C followed by hydrothermal synthesis at 80-200°C and 200 bar for 8h [75, 76]. However, kaolinisation requires the presence of granite in acid weathering of alkali feldspar into kaolinite but granite is rare on Mars. Nevertheless, other zeolites may be manufactured more readily and may be used to selectively absorb gases such as water vapour.

Most mineral processing methods are pyro- or hydro-metallurgical but both are less suited to recovery of low concentrations of metal in low grade ores as they result in a high gangue proportions. Ion exchange and solvent extraction are separation techniques more suited to dilute solutions. Ion exchange involves adsorption of metal ions to clay sorbents but clay has limited selectivity. Synthetic resins have replaced clays but their selectivities are still limited. Solvent extraction involves transferring metal ions in an aqueous phase to an organic solvent (kerosene and an organic chelating agent) with good selectivity. Hence, low concentration mineral processing will require the manufacture of sophisticated organics unless clays can be made to suffice in ion exchange. This offers the prospect of extracting rare earth metals in low concentrations. However, despite their utility for compact magnetic devices such as motors, we regard rare earth metal extraction as a downstream generation technology [77].

5 ADDITIVE MANUFACTURING

Once raw material feedstock – metal, plastic, ceramic, glass – has been extracted, it must be formed into useful components, assemblies and systems. Traditional subtractive manufacturing techniques such as forging, milling, grinding, turning, etc. all involve material waste (up to 90%) and wasted energy expended in frictional heating. Additive manufacturing minimises material waste compared with subtractive techniques and requires no jigs, fixtures, cutting tools or cooling fluids. It is a single-tool technique that minimises machining, welding, assembly and warehousing by tightly controlling the deposition of material. The characteristic of all additive manufacturing (3D printing) techniques is that they begin with a 3D CAD model of the component to be fabricated. This is sliced into 25 μm – 0.5 mm thick 2D cross-section layers to form an STL (standard tessellation language) file. STL files generate code that instructs the 3D printer nozzle to trace the shape of each layer of the object consecutively. Additive manufacturing involves the cumulative addition of these thin layers of material (typically ~50-100 μm) to build the 3D structures – a single machine can 3D print a multiplicity of 3D structures without specialised tooling. It is capable of manufacturing geometries unachievable by other methods, e.g. lattices are a favoured configuration to generate complex shapes but with minimum weight. 3D printed designs may be transmitted remotely so that products can be manufactured in-situ on demand – perhaps even from Earth to Mars. Mass production may be distributed to multiple locations where demand and raw material supply reside rather than implemented at a single supply source and then distributed to the locations of demand [78]. Manufacturing efficiency is enhanced through just-in-time (JIT) scheduling whereby fabricated parts are manufactured just in time for assembly to eliminate buffering and warehousing. This minimises wasted volume, wasted transport and infant obsolescence. The use of printing heads and/or powders permits the employment of multiple nozzles in parallel to fabricate in multiple materials including composite materials within the same manufacturing environment [79]. The chief problem with some 3D printing methods resides in rough surface finishing and poor tolerances. Total quality control (TQC) is essential which implies extensive use of measurement sensors during fabrication of every item to allow immediate corrective action.

Fused deposition modelling (FDM) has traditionally been applied to thermoplastics whereby a filament of such material is fed by rollers into a heated chamber, liquefied and extruded through a nozzle onto the work platform where it solidifies (e.g. Fig 2). A deposition head moves in the x-y plane to create the geometry while layering is implemented by the incrementally z-moving work platform. ABS softens at 100°C and flows at 200°C but decomposes at 250°C which define the viscosity limits for FDM using ABS. A multi-thermoplastic FDM system with two extrusion heads demonstrates the viability of multiple heads to print a model material and a sacrificial material within the same build process [80, 81]. FDM can also print elastomeric plastics and silicone plastics. FDM does not require post-processing. Comparatively low melting point Na_2O (32%)-SiO_2 (34%)-TiO_2 (29%)/B_2O_3 (5%) glass has also been 3D printed by extrusion [82]. Glass filaments were extruded at 1100°C from a purpose-designed resistively-heated insulated melt-extrusion nozzle of alumina (melting point of 1430°C) consuming 130 W of power. FDM-extruded thermoplastic may be modified with short glass fibres in the plasticiser to form 3D printed fibre reinforced composite of higher strength [83]. This represents a modification of the laminated object manufacturing (LOM) process which has employed multiple materials in discrete layers to form composites. FDM of metals using a metal liquid deposition head

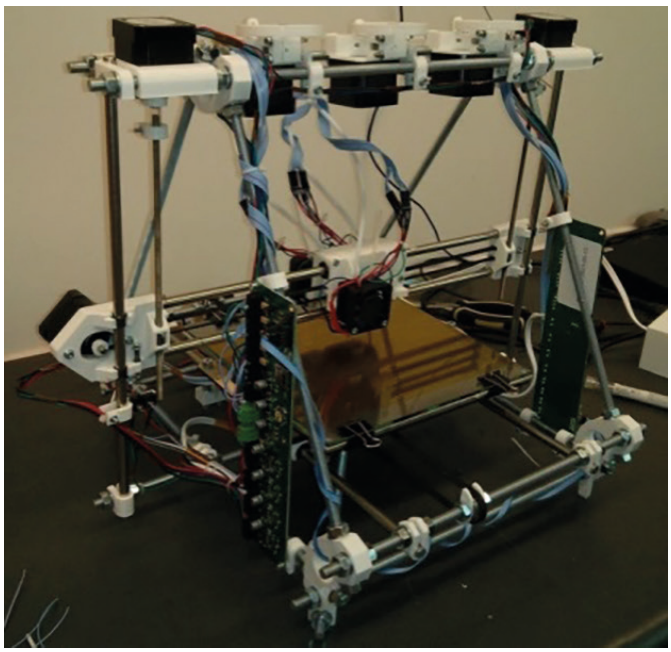

Fig.2 RepRap FDM printer.

requires low melting point metals in the range 210-220°C such as bismuth-tin alloys to build jigs, dies and soldered circuits [84]. They are, however, suited to limited application environments due to their low temperature tolerance.

Manufacturing of metals may be undertaken by 3D inkjetting a polyvinyl alcohol binder into a bed of ceramic powder such as mixtures of iron, nickel and cobalt oxides [85]. Following thermal processing to remove the binder, laser sintering and reduction to metal generates parts shrinkage of ~50%. The technique permits the construction of cellular structures such as trusses through 3D printing [86]. Alternatively, metal powder may be spread as a thin layer onto the work platform. Liquid plastic binder may be squirted to bind the powder into a solid. The powder may be melted using a laser or an electron beam which gives superior quality metal objects.

In selective laser sintering/melting (SLS/SLM), laser parameters such as lasing power, spot size, scanning speed and layer thickness are the prime determinants of the quality of parts produced. Beam speed determines both laser power and energy density delivered to the powder [87]. Laser power is given by:

$$P = \frac{v\rho dh(c(T_m - T_b) + Q_m)}{(1-R)} \quad (2)$$

where v = beam speed, ρ = powder density, c = specific heat, Q_m = latent melting heat, d = laser beam spot diameter, R = powder reflectivity, h = layer thickness, T_m = powder melting temperature, T_b = powder bed temperature. The bed temperature should be 3-4°C below the powder melting temperature. This aids in minimising non-uniform heating and cooling variations [88]. Laser energy density is given by:

$$E(cal/cm^2) = \frac{Pf}{vp} \quad (3)$$

where f = conversion factor, p = scan spacing <d. Tensile strength and densification increases with decreasing scan spacing and increased laser power. In laser engineered net shaping (LENS), a laser beam completely melts the powder which is fed into the laser beam by a nozzle rather than on a powder bed. SLS/SLM is capable of 3D printing metals, plastics, ceramics and glass. SLM of lunar regolith powder with 50 W of laser power at 1.07 μm in a 300 μm laser spot has been demonstrated for the construction of ceramic bricks with 40% porosity additively through 150 μm thick layers [89].

Electron beam additive manufacturing (EBAM) works with metal powders or rods and requires a high vacuum chamber (Fig 3). The electron beam generates a higher energy density and faster scanning speed than SLS. Electron beam melting is based on an electron gun with a tungsten filament heated to high temperatures to release electrons. The thermionically emitted electrons are accelerated in an electric field and focussed with electromagnetic coils within a vacuum environment. The highly focussed electron beam in a vacuum suffers from beam divergence due to mutual electrostatic repulsion at high currents but low energies. The electron beam melts either metal powder or metal rod into the desired 2D layer shape of 20-100 μm thickness (electron beam freeform fabrication approach adopts wire feedstock [90]). The melt depth (mm) is given by:

$$z = \frac{P}{10\Delta T\sqrt{kdv\rho c}} \quad (4)$$

where P = beam power (W), ΔT = temperature rise to melting point, k = thermal conductivity (W/mm°C), d = beam diameter (mm), v = beam velocity (mm/s), ρ = density (g/mm³), c = specific heat (J/g°C). EBAM prints parts that are fully dense without shrinkage. The high temperature provides for low residual stresses within the built part. Energy ~5 kW is generated by capacitor discharge to generate a beam current of up to 20 mA. X-ray generation is a potential hazard to human involvement but may be shielded. Metals that can be 3D printed include alloys of steel (including tool steel), copper, niobium, beryllium, nickel, aluminium, titanium, titanium-aluminium and nitinol. For the construction of electric motors (next section), metal materials required including wrought iron for motor structure, electrical steel for soft magnetic cores of motors and electromagnets, permalloy for magnetic shielding and fernico for electrical conducting wire coils. EBAM can potentially be combined with electric discharge machining (EDM) for complex machining, cavity excavation and finishing in a single machine. EDM is based on high voltage electric discharge from shaped electrodes.

Both SLM and EBAM yield fine microstructure due to rapid cooling rates – surface roughness is around 30-50 μm and unused powder may be recycled. Both SLM and EBAM are slow processes and build size is restricted by the chamber volume. Several 3D printing techniques can be used for concurrent machining including laser machining and electron beam machining. LENS (laser engineered net shaping) is an extension of laser-based additive manufacturing [91] in which hot iso-

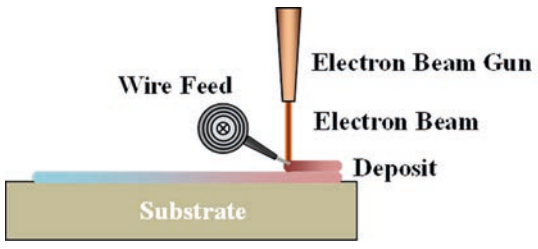

Fig.3 Electron beam additive manufacturing.

static pressing (HIP) at close to 1000°C for 4 h relieves surface stresses and porosity.

3D printing may also be employed to aid traditional material forming methods such as casting through the fabrication of moulds. 3D printing of flexible silicone enables moulds to be manufactured directly for casting [92]. Sand casting is commonly used for casting metal (investment casting) – a mould pattern is constructed from a sacrificial material (such as wax) which is inserted into sand mixed with clay, water and other additives for binding. Wax injection under pressure requires metal tooling. The ceramic mould is baked at 150-200°C and the sacrificial material removed. The ceramic mould is further hardened by firing. Molten metal is then poured into the ceramic cast while hot. Alternatively, regolith sand may be sintered directly into casts [93]. Sand may be mixed with sodium silicate which forms a very hard mould on passing CO_2 gas through it with laser sintering. The sodium silicate solution permeates the sand mould for a superior finish (it is also used as a gel sealant that hardens into a water-resistant cement). Sodium silicate may be obtained by dissolving silica sand in sodium carbonate at 1715°C: $xNa_2CO_3 + SiO_2 \rightarrow (Na_2O)_x.SiO_2 + CO_2$). Metal gears have been constructed from moulds of sand mixed with sodium silicate. The mould is broken to reveal the cast metal when solidified. Casting is less expensive than additive manufacturing and rapid 3D printing of moulds provides a mechanism to exploit the parallelisation of casting (rapid casting) with the versatility of 3D printing [94]. 3D printing of the mould from a wide variety of materials (such as silicone plastics) eliminates the requirement for metal tooling. ZCast is an exemplar method of 3D printing moulds for casting metals [95].

We envisage that the 3D printing facilities that will be required on Mars include FDM, EBAM and solar sintering/melting using solar concentrators. The difficulties in incorporating a laser into a self-replicating scheme and its poor conversion efficiencies render SLS/SLM as impractical for a first iteration self-replicator.

6 3D PRINTING MECHATRONIC COMPONENTS

The key to realising a self-replicating machine is the ability to 3D print electric motors and electronics. We hypothesise that if we can 3D print motors and electronics, we can 3D print any kinematic machine given the appropriate resources, energy and instruction procedure. If we can 3D print production machines, we can manufacture any product. Self-replicating machines have the potential to transform human Mars exploration in terms of both cost and risk. It is important to note that this first iteration of a self-replicating machine/universal constructor considers only systems that are circumscribed to systems that support self-replication and spacecraft construction – it does not consider issues associated with biological life support such as closed ecologically life support systems, space suits, food and medicine which are specialist capabilities.

Additive manufacturing may be supplemented with subtractive manufacturing. Shape deposition manufacturing (SDM) has been used to create homogeneous 3D structures layer-by-layer with internal cavities for pre-fabricated embedded components [96]. The internal cavities are typically milled into the 3D printed structure. The capacity to incorporate both embedded actuators and sensors and compliant materials was exploited to construct biomimetic structures like hexapodal legged robots [97]. Compliant materials (such as urethane), particularly at joints, work in conjunction with pre-fabricated actuators to store viscoelastic energy for zero-delay preflexes. These feedforward preflexes impart self-stability to perturbations without the time delays imposed by feedback loops. The embedded pre-fabricated sensors included Hall effect joint angle sensors, strain gauge force sensors, optical reflectance tactile sensors and piezoelectric polymers contact sensors [98]. However, in all these cases, the actuators and sensors were pre-fabricated for integration into 3D printed structures.

The holy grail of 3D printing is to print sensors, actuators, electronics and power systems in a single process to enable printing of robotic machines. Ionic polymer-metal composite (IPMC) actuators have been fabricated through multiple layer electrochemical processes as a type of freeform fabrication [99]. IPMC comprised Nafion films impregnated by metal particles – the layers are further electroplated to form electrodes. Nafion is a modified PTFE with perfluorinated sulphonate anion side branches. IPMC films bend in response to applied electric current/voltage but the result was inferior performance. Furthermore, they require complex manufacture so are not feasible from in-situ resources. Another possibility is the integration of self-assembly of micro-sensors on a substrate such as capillary-driven self-assembly of piezoelectric transducers [100]. This has yet to be explored. However, soft strain sensors with a gauge factor of 3.8 composed of carbon-based conductive ink within a passive elastomeric polymer have been 3D printed [101]. The ink, comprised of carbon particles in silicone oil, was extruded into the silicone elastomer through a deposition nozzle. A high resolution (~50 nm) capacitative position sensor with a parallel-plate configuration has also been inkjet-printed [102]. This demonstrates the feasibility of 3D printed RC elements for high resolution. We focus on 3D printing electric motors, but remark that electronics may be implemented using vacuum tubes which require a small set of materials – kovar wiring, tungsten cathode, metal oxide coatings, nickel anode and glass/ceramic enclosure.

Our initial venture into 3D printing electric motors began with 3D printing of the rotor – it comprised 50% iron particles by mass embedded in a polylactic acid (PLA) matrix 3D printed using a RepRap 3D printer (Fig 4a). The second aspect was to replace wire coils with photolithographically printed wire patterns (Fig 4b). Multiple layers of the wire patterns will be alternately integrated into the 3D printed rotor. The third and final aspect will be to 3D print permanent stator magnets – to date, we have replaced the original rare earth stator magnets with the same material as the rotor in a closed magnetic configuration with wire to form soft magnets (Fig 4c). These three components, when finalised, will yield the first fully printed general purpose DC electric motor. Once this has been demonstrated (we expect considerable challenges with the wire coils), we shall be exploring a means to reduce the current extensive manual assembly required. The challenge will be fabrication in multiple materials – the holy grail of 3D printing – required to construct an electric motor. A critical consideration is in tolerances which favours a 3D printing platform supplemented by an integrated milling head for high fidelity mating surfaces. The motor core will require alternating thin layers of silicon steel and ceramic/silicone with wire coils. We shall also explore the design space of 3D printed motors using genetic algorithms to exploit the manufacturing advantages offered by 3D printing.

Robotic mechanisms enabled by electric motors include powered machine tools, milling machines, lathes, 3D printers, rovers, manipulators, drills, etc. which can construct al-

most anything. This is the definition of a universal constructor which can manufacture copies of itself, thereby leveraging exponential productive capacity.

7 POWER SYSTEMS ON MARS

Solar energy generation on Mars is far weaker than that on the Earth or the Moon. Despite the diminished solar flux at the Martian surface of 300-500 W/m^2, most Mars exploration scenarios envisage photovoltaic power generation during daylight supported by battery or fuel cell power storage during the night. Furthermore, nuclear options cannot be accommodated within a first-generation self-replication system due to the requirement for exotic materials. Photovoltaic cells are a mature technology but atmospheric phenomena such as dust storms and cloud cover can severely degrade solar power systems. There are alternatives, however. Solar concentrators can heat fluid with solar dynamic conversion implemented through a turbine. This is around 25% efficient but they involve rotating machinery (using potentially 3D-printed motors as generators). Wind and geothermal power sources on Mars are unlikely to be practical. In a self-replicating machine context, power generation and storage must be implemented using only Martian resources. We proposed that solar concentrators such as Fresnel lenses or mirrors may be used to provide thermal energy focussed onto the cathodes of a bank of thermionic converters [103]. Mirrors are simpler to manufacture than Fresnel lenses – they require grinding on a motorised turntable. Russian space nuclear reactors offer thermionic conversion efficiencies of 15% which may be enhanced in several ways potentially yielding up to 50% conversion efficiencies [104]. Thermionic conversion is implemented through vacuum tube technology. Furthermore, energy storage may be implemented through flywheels which employ motors in a Halbach configuration. Most noteworthy is that the vacuum tube provides the basis for active electronics, electron beam additive manufacturing and energy generation while the electric motor provides the basis for general purpose actuation and power storage. This multirole re-use of components aids in the fundamental problem of closure in self-replication [105].

8 CONCLUSIONS

Self-replicating machines offer exponential growth in productive capacity. This exponential population growth suggests that evolutionary effects may yield loss of control of such machines. We have addressed this elsewhere and have determined that evolution can be effectively halted to any arbitrary degree using a combination of full redundancy and error detection and correction coding [106]. We have determined that a subset of raw materials available on Mars can supply all basic industrial functions required to support a human colony on Mars (excluding life support functions). Furthermore, that material subset suffices to build and implement a self-replicating architecture on Mars. The chemical processing architecture may be implemented through an industrial ecology thereby ensuring sustainability [107]. Crucial to self-replication is 3D printing, particularly of the mechatronic components required by robotic machines – actuators and electronics. We have almost achieved full demonstration of 3D printing electric motors as the first step to realising a self-replicating machine. Such a self-replicating architecture offers the most cost-efficient means of supporting a human colony – indeed, it can build the infrastructure required of such a colony including its power system. No Mars astronaut should leave home without his/her self-replicating machine.

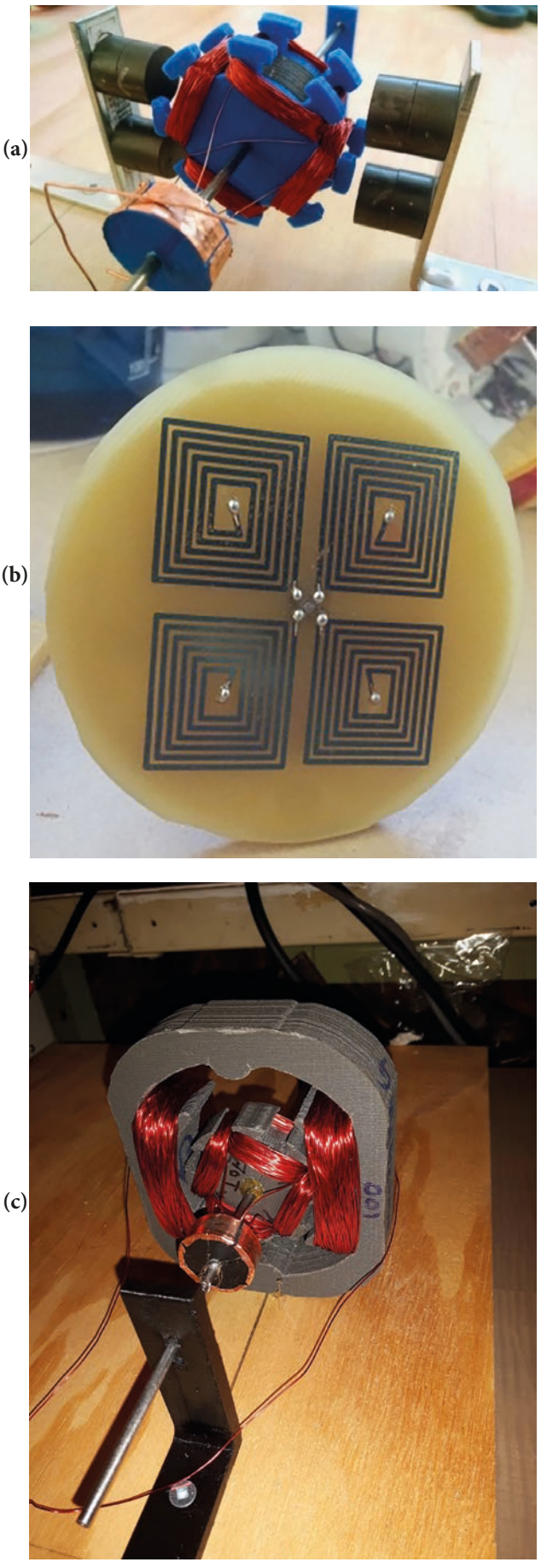

Fig.4 (a) 3D printed rotor for a DC motor with rare earth stator magnets; (b) photolithographically printed motor coil design; (c) 3D printed rotor and closed magnetic circuit stator with wire coils.

REFERENCES

1. L. Elkins-Tanton, "Rapid formation of Mars," *Nature*, Vol. 558, pp. 522-523, 2018.
2. T. Usui, "Martian water stored underground," *Nature*, Vol. 552, pp. 339-340, 2017.
3. Z. Dickeson, J. Davis, "Martian oceans," *Astronomy & Geophysics*, Vol. 61 (Jun), pp. 3.13-3.17, 2020.
4. M. Sephton, "Selecting Mars samples to return to Earth," *Astronomy & Geophysics*, Vol. 59, pp. 1.36-1.38, 2018.
5. A. Ellery, "Space exploration through self-replication technology compensates for discounting in NPV cost-benefit analysis – a business case?" *New Space J*, Vol. 5 (3), pp. 141-154, 2017.
6. B. Drake, "Human exploration of Mars: challenges and design reference architecture 5.0." *J Cosmology*, Vol. 12, pp. 3578-3587, 2010.
7. D. Craig, P. Troutman, N. Herrmann, "Pioneering space through the evolvable Mars campaign." *AIAA Space Conference and Exposition*, paper no 4409, 2015.
8. D. Landau, J. Longuski, "Comparative assessment of human-Mars mission technologies and architectures," *Acta Astronautica*, Vol. 65, pp. 893-911, 2009.
9. R. Moses, D. Bushnell, "Frontier in-situ resource utilisation for enabling sustained human presence on Mars," NASA TM-2016-219182, 2016.
10. M. Cross, A. Ellery, A. Qadi, "Estimating terrain parameters for a rigid wheel rover using neural networks," *J Terramechanics*, Vol. 50 (3), pp. 165-174, 2013.
11. D. Rapp, "Mars ISRU technology," in *Use of Extraterrestrial Resources for Human Space Missions to Moon or Mars*, Springer-Praxis Publishing, Heidelberg, pp. 31-90, 2013.
12. S. Starr, A. Muscatello, "Mars in situ resource utilization: a review," *Planetary & Space Science*, Vol. 182, 104824, 2020.
13. A. Baker, C. Tomatis, "ISRU in the context of future European human Mars exploration," *2nd World Space Congress, Houston*, IAA-02-IAA.13.3.08, 2002.
14. K. Sridhar, J. Finn, M. Kliss, "In-situ resource utilisation technologies for Mars life support systems," *Advances in Space Research*, Vol. 25 (2), pp. 249-255, 2000.
15. B. Parkinson, C. Cockell, J. Clarke, "In-situ resource use (ISRU) at pole station," in *Project Boreas: A Station for the Martian Geographic North Pole* (ed. Cockell C), British Interplanetary Society, pp. 57-61, 2006.
16. J. Wilson, et al., "Equatorial locations of water on Mars: improved resolution maps based on Mars Odyssey neutron spectrometer data," *Icarus*, Vol. 299, pp. 148-160, 2017.
17. M. Ralphs, B. Franz, T. Baker, S. Howe, "Water extraction on Mars for an expanding human colony," *Life Sciences in Space Research*, Vol. 7, pp. 57-60, 2015.
18. A. Hepp, G. Landis, C. Kubiak, "Chemical approach to carbon dioxide utilisation on Mars," *2nd Annual Symp University of Arizona/NASA Space Engineering Research Centre, Tucson, AZ*, pp. 799-816, 1991.
19. G. Landis, D. Linne, "Mars rocket vehicle using in-situ propellants," *J Spacecraft & Rockets*, Vol. 38 (5), pp. 730-737, 2001.
20. G. Landis, D. Linne "Acetylene fuel from atmospheric CO2 on Mars," *J Spacecraft* Vol. 29 (3), pp. 294-295, 1992.
21. R. Ash, W. Dowler, G. Varsi, "Feasibility of rocket propellant production on Mars," *Acta Astronautica*, Vol. 5, pp. 705-724, 1978.
22. K. Sridhar, M. Gottman, R. Baird, "2001 Mars in-situ oxygen production flight demonstration," *Proc 35th AIAA/ASME/SAE/ASEE Joint Propulsion Conf & Exhibit, Los Angeles, CA*, 1999.
23. K. Sridar, B. Vaniman, "Oxygen production on Mars using solid oxide electrolysis," *Solid State Ionics*, Vol. 93, pp. 321-328, 1997.
24. T. Simon, R. Baird, J. Trevathan, D. Clark, "Advanced in-situ resource utilisation (ISRU) production plant design for robotic and human Mars missions," *2nd World Space Congress, Houston, TX*, IAA-02-IAA.13.3.01, 2002.
25. C. McKay, T. Meyer, P. Boston, M. Nelson, T. MacCallum, O. Gwynne, "Utilising Martian resources for life support," in *Resources of Near-Earth Space* (ed. Lewis J, Mathews M, Guerrieri M), University of Arizona Press, Tucson, pp. 819-841, 1993.
26. J-K. Huang, M-T. Ho, R. Ash, "Expert systems for automated maintenance of a Mars oxygen production system," *J Spacecraft & Rockets*, Vol. 29 (4), pp. 425-431, 1992.
27. B. Salmi, "3D printing a rocket," *IEEE Spectrum*, (Nov), pp. 22-29, 2019.
28. S. Zhao, G. Siquerira, S. Drdova, D. Norris, C. Ubert, A. Bonnin, S. Galmarini, M. Ganobjak, Z. Pan, S. Brunner, G. Nystrom, J. Wang, M. Koebel, W. Malfait, "Additive manufacturing of silica aerogels," *Nature*, Vol. 584, pp. 387-392, 2020.
29. G. Chirikjian, Y. Zhou, J. Suthakorn, "Self-replicating robots for lunar development," *IEEE/ASME Trans Mechatronics*, Vol. 7 (4), pp. 462-472, 2002.
30. V. Zykov, E. Mytilinaios, B. Adams, H. Lipson, "Self-reproducing machines," *Nature*, Vol. 435, pp. 163-164, 2005.
31. R. Freitas, W. Gilbreath, *Advanced Automation for Space Missions*, NASA Conference Publication 2255, 1980.
32. J. von Neumann, A. Burkes, *Theory of Self-Reproducing Automata*, University of Illinois Press, Champaign, Illinois, 1966.
33. M. Snyder, J. Dunn, E. Gonzalez, "Effects of microgravity on extrusion based additive manufacturing," *AIAA Space 2013 Conference & Exposition*, paper no. 5439, 2013.
34. B. Khoshnevis, M. Bodiford, K. Burks, E. Thridge, D. Tucker, W. Kim, H. Toutanji, M. Fiske, "Lunar contour crafting – a novel technique for ISRU-based habitat development," *43rd AIAA Aerospace Meeting & Exposition, Reno NV*, paper no. 538, 2005.
35. R. Jones, P. Haufe, E. Sells, P. Iravani, V. Olliver, C. Palmer, A. Bowyer, "RepRap – the replicating rapid prototype," *Robotica*, Vol. 29 (1), pp. 177-191, 2011.
36. A. Ellery, "Are self-replicating machines feasible?" *AIAA J Spacecraft & Rockets,* Vol. 53 (2), pp. 317-327, 2016.
37. P. Metzger, A. Muscatello, R. Mueller, J. Mantovani, "Affordable, rapid bootstrapping of space industry and solar system civilization," *J Aerospace Engineering*, Vol. 26 (1), pp. 18-29, 2013.
38. C. McKay, "Scientific goals for Martian expeditions," *J British Interplanetary Society* Vol. 57, pp. 87-91, 2004.
39. B. Ehlmann, C. Edwards, "Mineralogy of the Martian surface," *Annual Reviews Planetary Science* Vol. 42, pp. 291-315, 2014.
40. V. Chevrier, P. Mathe, "Mineralogy and evolution of the surface of Mars: a review" *Planetary & Space Science*, Vol. 55, pp. 289-314, 2007.
41. I. Foster, P. King, B. Hyde, G. Southam, "Characterisation of halophiles in natural MgSO4 salts and laboratory enrichment samples: astrobiological implications for Mars," *Planetary & Space Science*, Vol. 58, pp. 599-615, 2010.
42. L. Schaefer, "Steamy proposal for Martian clays," *Nature*, Vol. 552, pp. 37-38, 2017.
43. M. West, J. Clarke, "Potential Martian mineral resources: mechanisms and terrestrial analogues", *Planetary & Space Science*, Vol. 58, pp. 574-582, 2010.
44. M. Coffin, O. Eldholm, "Large igneous provinces: crustal structure, dimensions and external consequences," *Reviews of Geophysics*, Vol. 32 (1), pp. 1-36, 1994.
45. A. Saunders, "Large igneous provinces: origin and environmental consequences," *Elements*, Vol. 1 (Dec), pp. 259-263, 2005.
46. B. Kading, J. Straub, "Utilising in-situ resources and 3D printing structures for a manned Mars mission," *Acta Astronautica*, Vol. 107, pp. 317-326, 2015.
47. H. Poisi, "Glass-ceramic production from lunar soils," *Space Resources News*, Vol. 6 (8), pp. 1-3, 1995.
48. B. Fabes, W. Poisl, "Processing of glass-ceramics from lunar resources," https://ntrs.nasa.gov/archive/nasa/casi.ntrs.nasa.gov/19910015067.pdf, 1991
49. G. Cesaretti, E. Dini, X. De Kestellier, V. Clla, L. Pambaguian, "Building components for an outpost on the lunar soil by means of a novel 3D printing technology," *Acta Astronautica*, Vol. 93, pp. 430-450, 2014.
50. L. Simonsen, J. Nealy, L. Townsend, J. Wilson, "Martian regolith as space radiation shielding," *J Spacecraft*, Vol. 28 (1), pp. 7-8, 1991.
51. G. Sanders, W. Larson, "Integration of in-situ resource utilisation into

lunar/Mars exploration through field analogues," *Advances in Space Research*, Vol. 47, pp. 20-29, 2011.

52. A. Matthews, "Magnetite formation by the reduction of haematite with iron under hydrothermal conditions," *American Mineralogist*, Vol. 61, pp. 927-932, 1976.
53. G. Landis, "Meteoritic steel as a construction resource on Mars," *Acta Astronautica,* Vol. 64, pp. 183-187, 2009.
54. K. Uchino, "Piezoelectric ultrasonic motors: overview." *Smart Materials & Structures*, Vol. 7, pp. 273-285, 1998.
55. Y. Bar-Cohen, S. Sherrit, B. Dolgin, N. Bridges, X. Bao, Z. Chang, A. Yen, R. Saund, "Ultrasonic/sonic driller/corer (USDC) as a sampler for planetary exploration," *Proc IEEE Aerospace Engineering Conf, paper no. 931716, Big Sky, MT*, 2001.
56. L. Sibille, A. Dominguez, "Joule-heated molten regolith electrolysis reactor concepts for oxygen and metals production on the Moon and Mars," *Proc 50th AIAA Aerospace Sciences Meeting, Nashville, TN*, AIAA 2012-0639, 2012.
57. L. Sibille, D. Sadoway, A. Sirk, P. Tripathy, O. Melendez, E. Standish, J. Dominguez, D. Stefanescu, P. Curreri, S. Poizneau, "Recent advances in scale-up development of molten regolith electrolysis for oxygen production in support of a lunar base," *Proc 46th AIAA Aerospace Sciences Meeting, Orlando, FL*, AIAA 2009-659, 2009.
58. A. Ellery, P. Lowing, P. Wanjara, M. Kirby, I. Mellor, G. Doughty, "FFC Cambridge process with metal 3D printing as universal in-situ resource utilisation," *Advanced Space Technology Robotics and Automation (ASTRA) Conf, Leiden, Holland*, 2017.
59. R. Navarro-Gonzalez, E. Vargas. J. de la Rosa, A. Raga, C. McKay, "Reanalysis of the Viking results suggests perchlorate and organics at midlatitudes on Mars," *J Geophysical Research*, Vol. 115 (E1), 2010JE003599, 2010.
60. H. Jahangiri, J. Bennett, P. Mahjoubi, K. Wilson, S. Gu, "Review of advanced catalyst development for Fischer-Tropsch synthesis of hydrocarbons from biomass derived syngas," *Catalytic Science & Technology*, Vol. 4, pp. 2210-2229, 2014.
61. T. Fini, C. Patz, R. Wentzel, "Oxidative coupling of methane to ethylene," *University of Pennsylvania Design Report Department of Chemical & Biomolecular Engineering*, CBE 64, 2014.
62. A. Vaccari, "Clays and catalysis: a promising future," *Applied Clay Sciences*, Vol. 14, pp. 161-198, 1999.
63. R. Robertson, "Clay minerals as catalysts," www.minersoc.org/pages/archive-CM/volume_0/0-2-47.pdf, 2006.
64. A. McAdam, M. Zolotiv, T. Sharp, L. Leshkin, "Preferential low pH dissolution of pyroxene in plagioclase-pyroxene mixtures: implications for martian surface materials," *Icarus*, Vol. 196, pp. 90-96, 2008.
65. G. Nagendrappa, "Organic synthesis using clay and clay-supported catalysts," *Applied Clay Science*, Vol. 53, pp. 106-138, 2011.
66. N. Kaur, D. Kishore, "Montmorillonite: an efficient, heterogeneous and green catalyst for organic synthesis," *J Chemical & Pharmaceutical Research,* Vol. 4 (2), pp. 991-1015, 2012.
67. A. Cabrera, M. Maple, S. Asunmaa, G. Arrhenius, "Formation of water and methane catalysed by lunar dust," NASA Report N91-71212, 1976.
68. T. Wogan, "Ceramics made stronger with 3D printing," *Chemistry World*, 11 Jan 2016.
69. R. Riedel, G. Mera, R. Hauser, A. Klonczynski, "Silicon-based polymer-derived ceramics: synthesis properties and applications – a review," *J Ceramic Society Japan*, Vol. 114, pp. 425-444, 2006.
70. R. Riedel, L. Toma, E. Janssen, J. Nuffer, T. Melz, H. Hanselka, "Piezoresistive effect in SiOC ceramics for integrated pressure sensors," *J American Ceramics Society*, Vol. 93 (4), pp. 920-924, 2010.
71. M. Sheppard, "Geopolymer composites: a ceramics alternative to polymer matrices," *Proc 105th Annual Meeting & Exposition of the American Ceramics Society*, 2007.
72. S. Cundy, P. Cox, "Hydrothermal synthesis of zeolites: history and development from the earliest days to the present time," *Chemistry Review*, Vol. 103, pp. 663-701, 2003.
73. C. Cundy, P. Cox, "Hydrothermal synthesis of zeolites: precursors, intermediates and reaction mechanism," *Microporous & Microporous Materials*, Vol. 82, pp. 1-78, 2005.
74. I. Petrov, T. Micjalev, "Synthesis of zeolite A: a review," http://conf.uni-ruse.bg/bg/docs/cp12/9.1/9.1-5.pdf, 2012.
75. E. Johnson, S. Arshad, J. Asik, "Hydrothermal synthesis of zeolite A using natural kaolin from KG Gading Bongawan Sabah," *J Applied Sciences*, Vol. 14 (23), pp. 3282-3287, 2014.
76. E. Johnson, S. Arshad, "Hydrothermally synthesised zeolites based on kaolinite: a review," *Applied Clay Science*, Vol. 97/98, pp. 215-221, 2014.
77. A. Ellery, P. Lowing, I. Mellor, M. Conti, P. Wanjara, F. Bernier, M. Kirby, K. Carpenter, P. Dillon, W. Dawes, L. Sibille, R. Mueller, "Towards in-situ manufacture of magnetic devices from rare earth materials mined from asteroids," *Proc Int Symp Artificial Intelligence Robotics & Automation in Space, Madrid, Spain*, paper no. 10c-1, 2018.
78. T. Campbell, C. Williams, O. Ivanova, B. Garrett, "Could 3D printing change the world? Technologies, potential and implications of additive manufacturing," *Strategic Foresight Report, Atlantic Council*, 2011.
79. E. Sachs, M. Cima, J. Cornie, D. Brancazio, J. Bredt, A. Curodeau, T. Fan, S. Khanuja, A. Lauder, J. Lee, S. Michaels, "3D printing: the physics and implications of additive manufacturing," *CIRP Annals – Manufacturing Technology*, Vol. 42 (1), pp. 257-260, 1993.
80. D. Espalin, J. Ramirez, F. Medina, R. Wicker, "Multi-material, multi-technology FDM system," *Solid Freeform Fabrication Symp, University of Texas, Austin*, pp. 828-834, 2012.
81. D. Espalin, J. Ramirez, F. Medina, R. Wicker, "Multi-material, multi-technology FDM: exploring build process variations," *Rapid Prototyping J,* Vol. 20 (3), pp. 236-244, 2014.
82. P. Wang, C. Chou, W. Wei, A. Liu, A. Wang, "Glass and hot extrusion by ME module for 3D additive manufacturing," *Proc IEEE Int Conf Industrial Technology, Tapei, Taiwan*, pp. 1167-1171, 2016.
83. W. Zhong, F. Li, Z. Zhang, L. Song, Z. Li, "Short fibre reinforced composites for fused deposition modelling," *Materials Science & Engineering A*, Vol. 301, pp. 125-130, 2001.
84, J. Mireles, D. Espalin, D. Roberson, B. Zinniel, F. Medina, R. Wicker, "Fused deposition modelling of metals," *Solid Freeform Fabrication Symp, University of Texas, Austin*, pp. 836-845, 2012.
85, C. Williams, D. Rosen, "Manufacturing metallic parts with designed mesostructured via 3D printing of metal oxide powder," *Proc Solid Freeform Fabrication Symp, University of Texas, Austin*, pp. 586-597, 2007.
86. C. Williams, J. Cochran, D. Rosen, "Additive manufacturing of metallic cellular materials via 3D printing," *Int J Advanced Manufacturing Technology*, Vol. 53, pp. 231-239, 2011.
87. I. Gibson, D. Shi, "Material properties and fabrication parameters in selective laser sintering process," *Rapid Prototyping J*, Vol. 3 (4), pp. 129-136, 1997.
88. A. Goulas, R. Friel, "3D printing with moondust," *Rapid Prototyping J*, Vol. 22 (6), pp. 864-870, 2016.
89. M. Chhabra, R. Singh, "Rapid casting solutions: a review," *Rapid Prototyping J*, Vol. 17 (5), pp. 328-350, 2010.
90. K. Taminger, R. Hafley, "Electron beam freeform fabrication (EBF3) for cost-effective near-net shape manufacturing," NASA TM 2006-214284, 2006.
91. C. Atwood, M. Griffith , L. Harwell, E. Schlienger, M. Ensz, J. Smugeresky, T. Romero, D. Greene, D. Reckaway, "Laser engineered net shaping (LENS): a tool for direct fabrication of metal parts," SAN098-2473C, 1998.
92. A. Rosochowski, A. Matuszak, "Rapid tooling: the state of the art," *J Materials Processing Technology,* Vol. 106, pp. 191-198, 2000.
93. X. Wan, J. Fuh, Y. Wong, Y. Tang, "Laser sintering of silica sand – mechanism and application to sand casting mould," *Int J Advanced Manufacturing Technology,* Vol. 21, pp. 1015-1020, 2003.
94. D. Bak, "Rapid prototyping or rapid production? 3D printing processes move industry towards the latter," *Assembly Automation*, Vol. 23 (4), pp. 340-345, 2003.
95. D. Bourell, T. Watt, D. Leigh, B. Fulcher, "Performance limitations in polymer laser sintering," *Physics Procedia*, Vol. 56, pp. 147-156, 2014.
96. L. Weiss, R. Merz, F. Prinz, G. Neplotnik, P. Padmanabhan, L. Schultz, K. Ramaswami, "Shape deposition manufacturing of heterogeneous structures," *J Manufacturing Systems*, Vol. 16 (4), pp. 239-248, 1997.
97. J. Cham, S. Bailey, J. Clark, R. Full, M. Cutkosky, "Fast and robust: hexapodal robots via shape deposition manufacturing," *Int J Robotics*

Research, Vol. 21 (10-11), pp. 869-882, 2002.

98. A. Dollar, C. Wagner, R. Howe, "Embedded sensors for biomimetic robotics via shape deposition manufacturing," *Proc 1st IEEE/RAS-EMBS Int Conf Biomedical Robotics & Biomechatronics*, paper no. 1639182, 2006.
99. E. Malone, H. Lipson, "Freeform fabrication of ionomeric polymer-metal composite actuators," *Rapid Prototyping J*, Vol. 12 (5), pp. 244-253, 2006.
100. J. Fang, K. Wang, K. Bohringer, "Self-assembly of PZT actuators for micropumps with high process repeatability," *J Microelectromechanical Systems,* Vol. 15 (4), pp. 871-878, 2006.
101. J. Muth, D. Vogt, R. Truby, Y. Menguc, D. Kolesky, R. Wood, J. Lewis, "Embedded 3D printing of strain sensors within highly stretchable elastomers," *Advanced Materials*, Vol. 26, pp. 6307-6312, 2014.
102. L-M. Faller, H. Zangl, "Feasibility considerations on an inkjet-printed capacitative position sensor for electrostatically actuated resonant MEMS-mirror systems," *IEEE J Microelectromechanical Systems*, Vol. 26 (3), pp. 559-568, 2017.
103. A. Ellery, "Solar power satellites for clean energy enabled through disruptive technologies," *Proc 23rd World Energy Congress (Award Winning Papers), Istanbul, Turkey*, pp. 133-147, 2016.
104. A. Ellery, "In-situ resourced solar power generation and storage for a sustainable Moon Village," *Int Astronautics Congress, Washington DC*, IAC-19,C3.4.4.x49639, 2019.
105. Freitas R, Merkle R, *Kinematic Self-Replicating Machines*, Landes Bioscience, Texas, 2004.
106. A. Ellery, G. Eiben, "To evolve or not to evolve: that is the question," *Proc Artificial Life Conf*, pp. 357-364, 2019.
107. A. Ellery, "Sustainable in-situ resource utilisation on the Moon," *Planetary & Space Science*, Vol. 184, 104870, 2020.

Received 02 May 2020 **Approved** 22 October 2020